

A Miniaturized In Situ Tensile Platform under Microscope

Zhichao Ma, Hongwei Zhao*, Hu Huang, Kaiting Wang, Qinchao Li, Xiaoqin Zhou, Xiaoli Hu

College of Mechanical Science and Engineering, Jilin University
Renmin Street 5988, Changchun, Jilin 130025, China, telp+86-0431-85095428
e-mail: kobe2324@126.com, hwzhao@jlu.edu.cn*, huanghuzy@163.com, 659667638@qq.com,
shizhelee@qq.com, xqzhou@jlu.edu.cn, 253163882@qq.com

Abstrak

Tujuan pengujian mekanik pada spesimen tiga dimensi dengan ukuran fitur pada tingkat sentimeter, sebuah platform tarik miniatur, yang menyajikan kompatibilitas dengan pemindai mikroskop elektron (SEM) dan mikroskop metalografi, dirancang dan dibangun. Platform ini dapat secara akurat mengevaluasi parameter seperti modulus elastisitas, pemanjangan dan batas hasil, dan lain-lain. Eksperimen kalibrasi sensor beban dan sensor pergeseran menunjukkan dua jenis sensor memiliki linearitas yang tinggi. Pengujian galat transmisi dan parameter modal menunjukkan bahwa platform ini memberikan perilaku ikutan dan pemisahan wilayah resonansi yang baik. Pengujian perbandingan berbasis kurva tegangan-regangan dilakukan antara platform buatan sendiri dan instrumen tarik komersial (Instron) untuk memverifikasi kelayakan platform. Lebih lanjut, eksperimen tarik asli di bawah mikroskop metalografi dilakukan pada jenis baja mangan.

Kata kunci: *in situ testing, kurva tegangan-regangan, SEM, tensile*

Abstract

Aiming at the mechanical testing of three-dimensional specimens with feature size of centimeter level, a miniaturized tensile platform, which presents compatibility with scanning electron microscope (SEM) and metallographic microscope, was designed and built. The platform could accurately evaluate the parameters such as elastic modulus, elongation and yield limit, etc. The calibration experiments of load sensor and displacement sensor showed the two kinds of sensors had high linearity. Testing of transmission error and modal parameters showed that the platform presented good following behaviors and separation of resonance region. Comparison tests based on stress-strain curve were carried out between the self-made platform and the commercial tensile instrument (Instron) to verify the feasibility of the platform. Furthermore, the *in situ* tensile experiment under metallographic microscope was carried out on a kind of manganese steel.

Keywords: *in situ testing, SEM, stress-strain curve, tensile*

1. Introduction

The processes of crack initiation, propagation, deformation until fracture of materials could be researched via *in situ* testing based on the observation of SEM, metallographic microscope, X-ray diffraction and Raman spectrometer, etc [1-3]. Frequently, the *in situ* tensile testing could be adopted as primary method to deeply investigate the micro-mechanical behavior of various materials combined with the engineering stress-strain curve [3], [4]. Lawrence Livermore National Laboratory (LLNL) and Lawrence Berkeley National Laboratory (LBNL) researched on nanotubes, nanowires and many other specimens with extremely tiny dimensions based on FIB technology under uniaxial tensile mode [2], [5], [6]. C. J. Bettles [2] of Monash University and D. Q. Zhang [3] of Dalian University of Technology constructed tensile platforms with CCD imaging component respectively. In addition, these works were mostly developed based on MEMS technology [6], [7].

In situ tensile testing based on AFM was also frequently selected, such as T. Nishino [4] of Kobe University developed a device based on the functions of manual and automatic adjustment for the tensile testing of PET film material. With the financial aid of famous DURINT plan, E. Bamberg [5] of MIT investigated an electromechanical controlled device driven by stepping motor, the tensile force, transmitted by synchronous belt and ball-screw, can achieve a maximum value of 25N with resolution of 125mN. Z. Qin [6] of Harbin Institute of Technology

designed and fabricated a platform for the testing of magnetic tape film, the maximum tensile force can reach 200N with displacement resolution of $10\mu\text{m}$. However, vast majority of these works researched on thin film materials and as limited by measuring principle and imaging speed of AFM, it was difficult to deeply reveal the relationships between the mechanical behaviors and mechanism of deformation, damage of materials by means of discontinuous observation.

In situ tensile testing inside SEM for the three-dimensional specimen with macroscopic dimensions, representative research works restricted to M. Aboulfaraj [7] of CNRS, R. Rizzieri [8] and K. I. Dragnevski [9] of Cavendish Lab. M. Aboulfaraj developed a compact platform with functions of uniaxial tension and pure shear inside JEOL SEM 810. Meanwhile, the platform could solely provide qualitative calibration without the capability of collecting the force/displacement signals, which was integrant for drawing the engineering stress-strain curves and ensuring the elastic modulus and yield stress, etc. R. Rizzieri of Cavendish Lab developed a platform with maximum tensile force of 200N for investigating the deformation process of biological polymer materials, the load was produced by combination of stepping motor, gear pair and ball-screw. Owing to the rectilinearly series connection of force sensor, specimen grippers, gear reducer and stepping motor, relative long structure distribution weakened the system stiffness. To achieve the in situ tensile system for the testing of specimen with feather with feature size of centimeter level inside SEM with miniaturized chamber and strict working distance, miniaturized structure and loading capacity were required to be rationally matched [9], [10].

This paper proposed a miniaturized platform with minimum dimensions of $105\text{mm}\times 95\text{mm}\times 34\text{mm}$ for in situ tensile testing, which presented excellent compatibility with MA-2003I metallographic microscope and Hitachi TM-1000 SEM. Both the load and displacement signals could be real-timely measured to form the engineering stress-strain curve. The calibration experiments of load and displacement sensors were carried out, testing of transmission error and modal parameters showed that the platform presented good following behaviors and separation of resonance region, comparison tests on stress-strain curve were carried out between the self-made device and the commercial tensile instrument (Instron). Finally, the in situ tensile experiment under metallographic microscope was carried out on a kind of manganese steel.

2. Design of the platform

2.1. Functional design

Structure diagram of the proposed platform is shown in Figure. 1, the servo motor, combined with reducer with large reduction ratio, was selected as precise driving unit. Two-stage worm gear and a small lead ball-screw constituted the transmission unit for achieving the linear motion. Via the control mode of pulse/direction for the servo motor, the platform could provide quasi-static loading mode with ultra-low speed of $0.1\mu\text{m/s}$, additionally, the ball-screw and worm gear could achieve self-locking function to facilitate the imaging with high resolution as the device could momentarily stop before imaging. Entire technical parameters of the platform are shown as follows: minimum dimensions of $105\text{mm}\times 95\text{mm}\times 34\text{mm}$, displacement resolution of $1\mu\text{m}$, tensile stroke of 10mm, maximum load of 1000N, load resolution of 0.5N, maximum specimen dimension of $16\text{mm}\times 3\text{mm}\times 1\text{mm}$. To solve the alignment issues, the location relationship between the specimen and the grippers was realized by a pair of grooves of the grippers, which presented the same shape with the rectangular cross section of the specimen.

In situ testing system inside Hitachi TM-1000 SEM is shown in Figure. 2. The Hitachi TM-1000 SEM presents a chamber with diameter of 140mm and working distance of 3.5mm, with which the proposed platform could easily realize the structure compatibility. Combined with the stage of the SEM, the concerned areas of the specimen, such as areas of potential crack initiation or joint surface between the matrix and thin film, could be deeply observed with high magnification. Meanwhile, as the load sensor, displacement sensor and servo motor were far enough away from the beam to affect it, therefore, the electromagnetic compatibility with the SEM was solved, although these components present a certain magnetic sensitivity. To facilitate the control of the proposed platform, the shielding wires of servo motor, load sensor and displacement sensor were educed outside the vacuum chamber through the interfaces

embedded inside the sealed door of the SEM. Control command of square-wave signal was created from the motion control card (ART-PCI 1010) then sent to servo motor (Maxon Ec-max22), which then produces accurate angular displacement and finally turn into ultra-low linear motion through the precise transmission unit. Load and displacement signal is measured by the commercial load sensor and displacement sensor respectively. Furthermore, the analog signal of load or displacement could be selected as feedback sources for precisely closed loop control of the in situ testing system. Additionally, based on the optimized proportional integration (PI) parameters, pulse/direction mode was selected for driving the servo motor. The software is used to record the data from data acquisition card (ART-PCI 8602), and the observation interface is displayed on computer. In addition, all high-power circuits are separated from the low-power devices to minimize electrical noise and ensure safety.

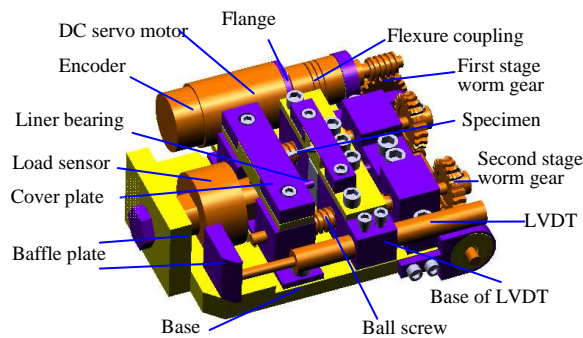


Figure 1. Structure diagram of the platform

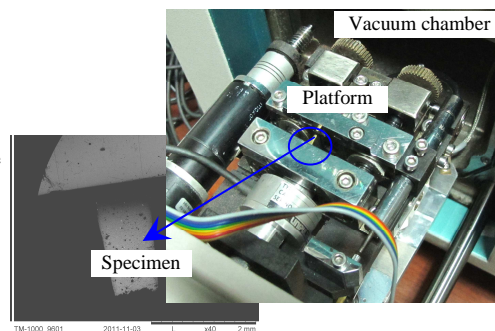


Figure 2. In situ tensile system under SEM

2.2. Finite element analysis of the grippers

Material of 40Cr, whose strength, hardness and fatigue strength were extremely increased via process of high frequency quenching, was adopted for the gripping of the specimen. For the finite element analysis, the contact region of the gripper was refined with tiny girds. Figure. 3 shows the stress distribution of single gripper when tensile force of 1000N was applied on the contact region. Maximum stress of 199.038MPa of the gripper was obtained. As material of 40Cr, with yield stress σ_s of 785Mp, was adopted as matrix material, the gripper would not present yield phenomenon or plastic deformation. Furthermore, to avoid resonance phenomenon during tensile testing as well as to ensure the stability of the platform, modal analysis via finite element method was necessarily carried out. Seen from Figure. 4, the first order mode frequency of single gripper was about 5123Hz, which is by far higher than the normal working frequency of the platform.

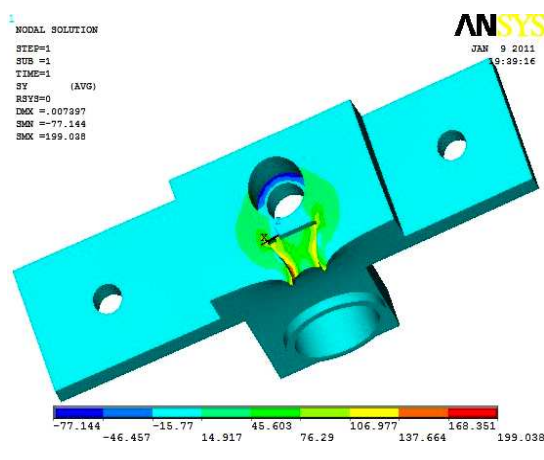


Figure 3. Stress distribution

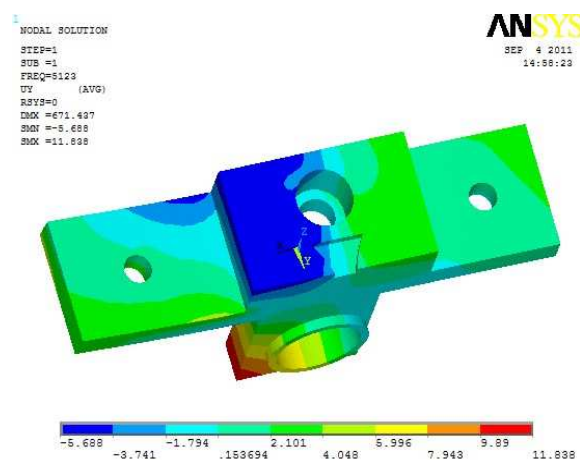


Figure 4. Modal shapes

3. Experiments and discussions

3.1. Calibration of sensors

Mechanical parameters of materials, such as elastic modulus, yield strength, tensile strength and elongation, are mainly obtained from the load-displacement ($F-l$) curve, which is drawn by load and displacement data from load and displacement sensors. Therefore, calibration experiments were necessarily carried out to evaluate the linearity of sensors. The load sensor is from Unipulse with a range of 100kg and resolution of 0.5N. LVDT-type displacement (LVDT) is from Volfa with a range of ± 10 mm and resolution of $1\mu\text{m}$. Figure. 5 and Figure. 6 are the calibration results of the LVDT and the load sensor, respectively. From these two figures, relation between displacement l (mm) and output voltage X_1 (V) is $l = 19985 \times X_1 - 0.654$, and relation between load F (N) and output voltage X_2 (V) is $F = -215.05 \times X_2 + 118.385$. Their linear correlation coefficients R^2 are both close to 1, which indicates that both the LDVT and the load sensor have high linearity.

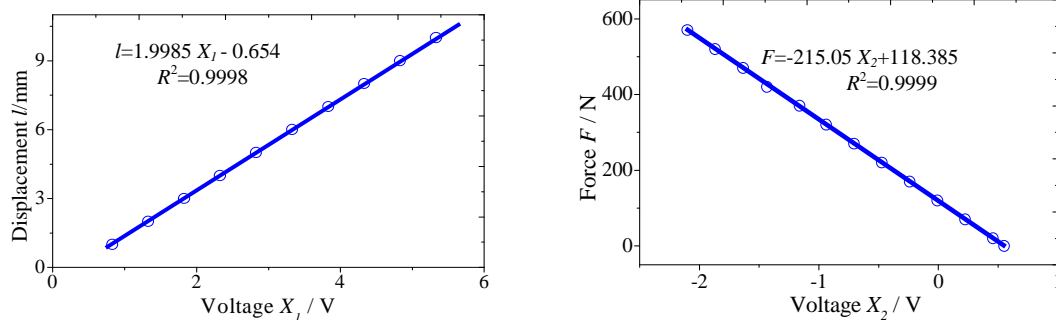


Figure 5. Calibration result of displacement sensor Figure 6. Calibration result of load sensor

3.2. Testing of transmission performance

The established system for output performance test of the platform is shown in Figure. 7. The motion of gripper A was directly detected by non-contact laser sensor (LK-G10) with rapid response and a resolution of 10nm. Meanwhile, the calibration displacement measured by the photoelectric encoder (HEDL9140-1000) was put forward to be compared. Therefore, the transmission performance of the platform was estimated by calculating the difference of the two displacements as the transmission error. With various loading speeds of $5\mu\text{m/s}$, $10\mu\text{m/s}$ and $20\mu\text{m/s}$, the displacement differences detected by the laser sensor and photoelectric encoder during the loading process were obtained. As shown in Figure. 8, the corresponding transmission errors were shown as $2.03\mu\text{m}$, $3.86\mu\text{m}$ and $6.36\mu\text{m}$, the errors were mainly caused by the acceleration process of the servo motor and the gap of transmission unit. As the loading speed increased, the transmission error presented tendency of increasing. In addition, the platform presents favorable transmission performance behaviors when the loading speed is lower than $5\mu\text{m/s}$, which meets the requirement of quasi-static loading mode as above mentioned.

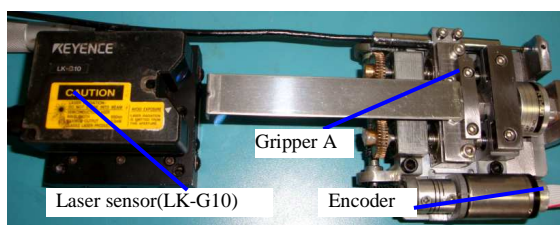


Figure 7. Transmission performance test

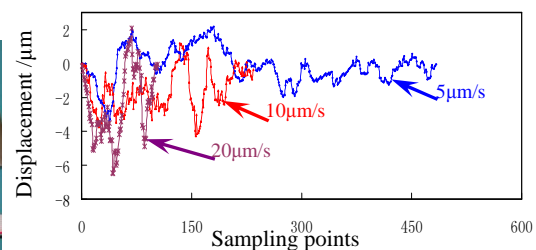


Figure 8. Testing of transmission error

3.3. Testing of modal parameters

The given sweep frequency for modal testing, generated from arbitrary waveform generator (RIGOL) with wave form of sinusoidal or square, was the excitation signal for activating the electromagnetic exciter. Meanwhile, high frequency laser doppler vibration tester (VibroMET) was used for the testing of modal frequencies in order to evaluate the dynamic properties of the platform. The diagram of the modal test system is shown in Figure. 9 (a).

As shown in Figure. 9 (b), frequencies of the flexure coupling were detected when applied strain speeds of $10\mu\text{m/s}$ and $20\mu\text{m/s}$, the corresponding testing frequencies were 11Hz and 21.9Hz respectively, which accord with the rotational speed of the servo motor. Therefore, with the forced vibration caused by the normal motion of the servo motor, the platform presented a working frequency below 50Hz. Furthermore, during the harmonic response test, the given sweep frequency with range from 10Hz to 5000Hz, was used for the testing of modal frequencies. Figure. 9 (c) shows that the natural frequencies of the first two modal shapes were 225.9Hz and 3244.6Hz, which were by far higher than the actual working frequency of the platform. Therefore, the platform could avoid the resonance region with maximum strain speed below $100\mu\text{m/s}$. As above mentioned, quasi-static loading mode accords with the requirement of in situ observation, thus, the platform presented favorable stability at normal working condition.

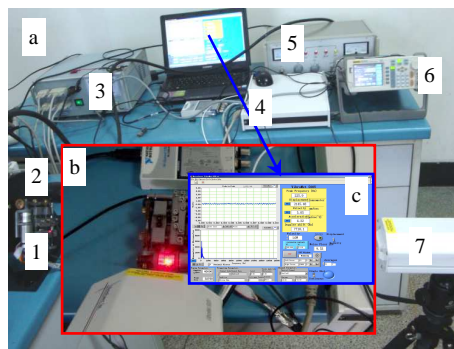


Figure 9. Diagram of modal test system: 1 expresses the tensile platform, 2 is the electromagnetic exciter, 3 is the multi-channel servo controller, 4 is the data acquisition module of laser doppler vibration tester, 5 is the power amplifier of electromagnetic exciter, 6 is the arbitrary waveform generator (RIGOL) and 7 is the laser generator of high frequency laser doppler vibration tester (VibroMET)

3.4 Feasibility of the platform

For plate specimen, it was understood that simple geometries allow easy and accurate extraction. Plate specimen with a rectangular cross section could be adopted as the macroscopic stress concentration, which would cause the specimen to fail prematurely and invalidate the result of the testing, could be avoided. Before testing, processes of wire cutting and single side polishing of the specimen were required to ensure the microstructure distinct, schematic of the gripping way with illustrations of the specimen's size is shown in Figure. 10.

The engineering stress-strain curves of 45# were obtained by the self-made platform to be compared with commercial tensile instrument (Instron) with the same experimental conditions. In order to reduce the error, five tensile experiments by each instrument were conducted.

As shown in Figure. 11, the reference curve was from the commercial tensile instrument, and the tested curve was from directly detected force and displacement signal of the self-made platform. Seen from the curves, the tested curve approximately coincided with the reference curve. Furthermore, the mechanical parameters of 45# obtained by each instrument are shown in Table. 1, the average value of the corrected elastic modulus E of 203.58GPa, the average value of the corrected tensile strength σ_b of 605.54MPa and the average value of the corrected elongation δ of about 16.12% were obtained by the self-made device. Meanwhile, for commercial tensile instrument, these parameters show corresponding values of 205.08GPa, 605.86MPa and 15.72%, respectively. Therefore, all the corrected parameters are close to the experimental values obtained by commercial tensile instrument, which preliminarily indicates the feasibility of the platform.

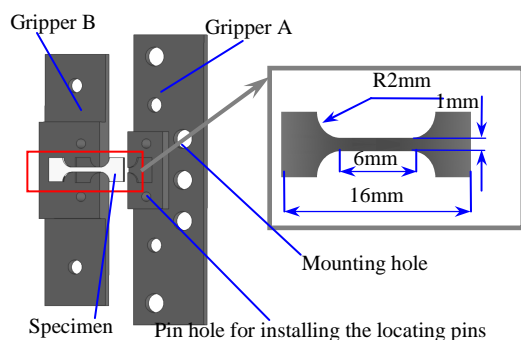


Figure 10. Schematic of the gripping way the specimen's size

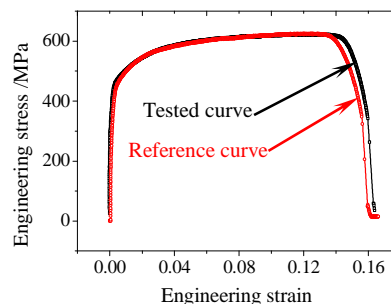


Figure 11. Comparison results

Table 1. Comparison results of parameters between the commercial instrument and our self-made platform

	Commercial instrument			Self-made platform		
	E (GPa)	σ_b (MPa)	δ (%)	E (GPa)	σ_b (MPa)	δ (%)
1	204.6	604.6	15.6	203.6	604.8	16.2
2	206.5	606.3	15.8	202.4	605.2	16.1
3	207.5	607.2	15.4	203.4	606.2	16.1
4	206.2	605.4	16.1	203.7	604.4	15.8
5	204.8	605.8	15.7	204.8	607.1	16.4
Mean	205.08	605.86	15.72	203.58	605.54	16.12

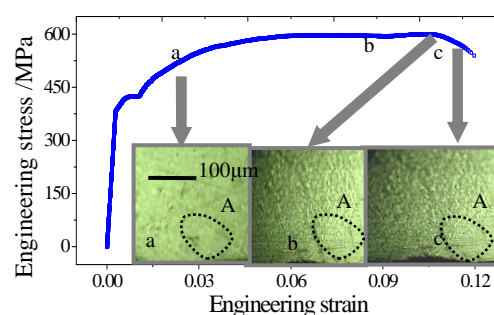


Figure 12. Stress-strain curve and microscope images of deformation process of a kind of manganese steel

3.5 In situ tensile testing under microscope

The in situ tensile testing takes advantage of avoiding elastic recovery when the device momentarily stops before imaging. Metallographic microscope (MA 2003I) with high resolution digital imaging system was adopted to observe the processes of deformation, damage until fracture of a kind of manganese steel. The engineering stress-strain curve and corresponding metallographic microscope images of the steel surfaces for applied tensile stresses higher than their nominal yield stress were timely record as shown in Figure. 12.

Seen from the microscope images of the steel surfaces for applied tensile stresses at stages of yield stress, maximum stress and necking, when the engineering stress increased to 483MPa, abundant distinct micro voids were observed as sources of crack initiation(region A in Figure 12, for instance). When the engineering stress increased to 603MPa, apparent necking phenomenon appeared. As uniaxial stress increases, those cracks continually expand and the cracks propagation spread along shear bands at an angle of approximate 45degree to the direction of tensile axis. Obvious shear fracture mode was found, and the necking phenomenon occurred in the region close to the cross section. Principal shear stress lead to the slip at an angle of approximate 45degree to the direction of the tensile axis, the ultimate fracture presents apparent shearing type.

4. Conclusion

This paper proposed a miniaturized platform for in situ tensile testing with minimum dimensions of 105mm×95mm×34mm, the platform could provide maximum tensile load of 1000N and could be compatible with MA-2003I metallographic microscope and Hitachi-TM-1000 SEM. The calibration experiments showed the load sensor and displacement sensor had high linearity and stability. Test of transmission error and modal parameters showed that the platform presented good following behaviors and separation of resonance region. The engineering stress-strain curves of 45# were obtained by the self-made platform to be compared with

commercial tensile instrument (Instron) with the same experimental conditions. The average value of the calibrated elastic modulus E , tensile strength σ_b and elongation δ were close to the experimental values obtained by commercial tensile instrument, which preliminarily indicates the feasibility of the corrected methods. Mechanisms of crack initiation, propagation and fracture of a kind of manganese steel were investigated via in situ observation under metallographic microscope, the self defects act dominating effect to lead to crack initiation. Furthermore, shear stress lead to the expansion of main crack along the slip band, crack propagation spread along shear bands at an angle of approximate 45degree to the direction of tensile axis, and the ultimate fracture presents apparent shearing type.

Acknowledgements

This research is funded by the National Natural Science Foundation of China (Grant No. 50905073, 51105163), National Hi-tech Research and Development Program of China(863 Program) (Grant No. 2012AA041206), Key Projects of Science and Technology Development Plan of Jilin Province (Grant No. 20110307) and International Science and Technology Cooperation Program of China (Grant No. 2010DFA72000).

References

- [1] Neelakantan L, Schönberger B, Eggeler G, Hassel, A W. An in situ tensile tester for studying electrochemical repassivation behavior: Fabrication and challenges. *Review of Scientific Instruments*. 2010; 81(3).
- [2] Bettles C J, Lynch P A, Stevenson A W, Tomus D, Gibson M A, Wallwork K, Kimpton J. In situ observation of strain evolution in Cp-Ti over multiple length scales. *Physical Metallurgy and Materials Science*. 2011; 42: 100-110.
- [3] Zhang D Q, Chu J G, Hou Z W, Wang L D. An off-chip actuated tensile test device for microscale mechanical testing. *Chinese Journal of Mechanical Engineering*. 2009; 20.
- [4] Nishino T, Hirao K, Kotera M, Nakamae K, Inagaki H. Kenaf reinforced biodegradable composite. *Composites Science and Technology*. 2003; 63: 1281–1286.
- [5] Bamberg E, Grippo C P, Wanakamol P, Slocum A H, Boyce M C, Thomas E L. A tensile test device for in situ atomic force microscope mechanical testing. *Precision Engineering*. 2006; 30: 71-84.
- [6] Tu H, Cheng J, Chang Q, Zhou Q, Wang J, Zhang G, Fang F. Growth and stress analysis of necks for 300 mm CZ silicon single crystals. *Microelectronic Engineering*. 2001; 56: 89-92.
- [7] Aboulfaraj M, G'Sell C, Ulrich B. In situ observation of the plastic deformation of polypropylene spherulites under uniaxial tension and simple shear in the scanning electron microscope. *Polymer*. 1995; 36: 731-742.
- [8] Rizzieri R, Mahadevan L, Vaziri A, et al. Superficial wrinkles in stretched, drying gelatin films. *Langmuir*. 2006; 22: 3622-3626.
- [9] Rizzieri R, Baker F S, Donald A M. A tensometer to study strain deformation and failure behavior of hydrated systems via in situ environmental scanning electron microscopy. *Review of Scientific Instruments*. 2003; 74: 4423-4428.
- [10] Stokes D J, Donald A M. In situ mechanical testing of dry and hydrated breadcrumb in the environmental scanning electron microscope (ESEM). *Journal of Materials Science*. 2000; 35: 599-607.